

^{26}Al in Galaxy Regions: Massive-Star Interactions with the ISM

R. Diehl ^a, M. Cerviño ^b, D.H. Hartmann ^c, and K. Kretschmer ^a

^a*Max-Planck-Institut für extraterrestrische Physik, D-85741 Garching, Germany*

^b*Instituto de Astrofísica de Andalucía (CSIC), E-18080, Grenada, Spain*

^c*Clemson University, Clemson, SC 29634-0978, USA*

Abstract

Galactic ^{26}Al is believed to be predominantly injected into the ISM from winds and supernovae of massive stars. These stars are typically born in groups and associations, which evolve over tens of Myrs, and shape the interstellar environment in their surroundings. ^{26}Al contained in stellar outflows produces a gamma-ray line at 1.809 MeV, which is potentially observable from regions of active star formation on time scales of a few Myrs, i.e., comparable to the mean life of ^{26}Al . This relatively long time scale may lead to spatial offsets between the observed ^{26}Al gamma-ray emission and tracers of ^{26}Al sources, such as locations of massive-stars, HII regions, or IR emission from dust heated by starlight. We find evidence for such an offset in star forming regions towards Orion.

Key words: stars: late stages of evolution, nucleosynthesis, nuclear processes (astrophysics), Interstellar matter: Milky Way

PACS: 97.60, 97.10.C, 26.20, 26.30, 95.30.C, 98.38

1 Gamma-Ray Line Emission from ^{26}Al , and source populations

^{26}Al was discovered in the interstellar medium of our Galaxy by the HEAO-C instrument (Mahoney et al., 1982), and since then has been observed with many gamma-ray telescopes from high-altitude balloons or spacecraft (for a review see Prantzos and Diehl, 1996, and recent measurements in (Smith, 2003; Diehl et al., 2003)). Especially the all-sky image of ^{26}Al emission derived from 9 years of COMPTEL measurements with the Compton Observatory (Oberlack, 1997; Plüschke, 2001) demonstrated that ^{26}Al emission is diffuse in nature, extended along the Galactic plane, and especially bright in regions with

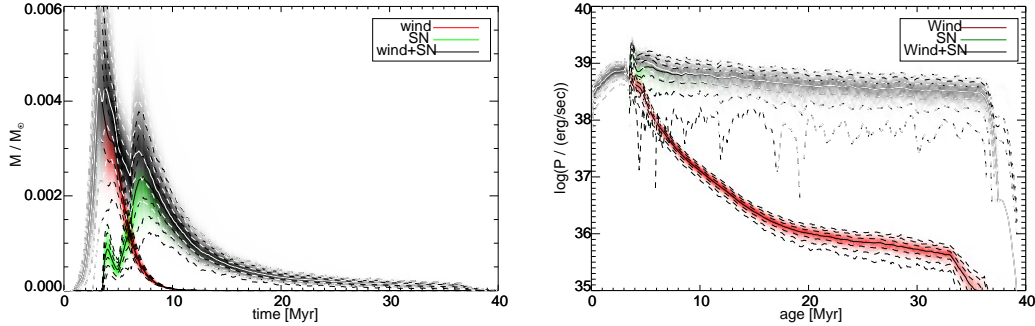


Fig. 1. Monte Carlo simulations of the evolution of clusters with 100 massive stars: Time evolution of the ^{26}Al mass (left) due to the balance between injection (from winds and SNe) and decay, and the associated (kinetic) energy injection rate (right). Gray scale profiles indicate probability densities obtained from simulations of many such clusters.

enhanced numbers of massive stars. Emission which is even more widely spread-out on the sky (e.g., local and nearly isotropic) is suggested by systematically-larger flux values obtained with non-imaging, large field-of-view instruments such as SMM, GRIS, and RHESSI.

Massive stars with their short lifetimes (1-10 Myr) occur in groups, and are preferentially associated with spiral-arms of the Galaxy (e.g. Efremov and Elmegreen, 1998). Their spatial distribution is uncertain beyond ~ 2 kpc due to severe extinction (Russeil, 2002; van der Hucht, 2002), but OB star groups have been mapped in remarkable detail in the solar vicinity (Blaauw, 1964; de Zeeuw et al., 1999). The Gould Belt (Pöppel, 1997) probably outlines a local region of star formation that was active during the past ~ 30 –60 Myr, with about a dozen identified OB associations lined up on its circumference (Perrot and Grenier, 2003) within ~ 500 pc of the sun. Massive-star concentrations appear at prominent lines-of-sight, such as the Cygnus region [$75^\circ < l < 100^\circ$], the Vela region [$260^\circ < l < 270^\circ$], the Anticenter region [$170^\circ < l < 210^\circ$], and the Sco/Cen region [$300^\circ < l < 360^\circ$] with its closest stars at ~ 140 pc. But even for such nearby regions, one expects incompleteness of the massive-star census from intervening interstellar clouds, as demonstrated for Cyg OB2 with a detailed mapping in the IR (Knödlseder, 2000).

Primary ^{26}Al candidate source populations related to massive stars are Wolf Rayet stars and core-collapse supernovae (Prantzos and Diehl, 1996). It is difficult, however, to distinguish their relative contributions. Arguments for a dominating Wolf Rayet star contribution were derived from comparisons with free-electron emission (Knödlseder, 1999a). But the absence of a signal from the nearby (260pc) $\gamma^2\text{Vel}$ system with its WR-11 star does not support this interpretation (Oberlack et al., 2000). Also, the detection of ^{60}Fe gamma-ray emission by RHESSI (Smith, 2003) from the inner Galaxy, which is a prominent ^{26}Al source region, argues for a significant ^{26}Al contribution from

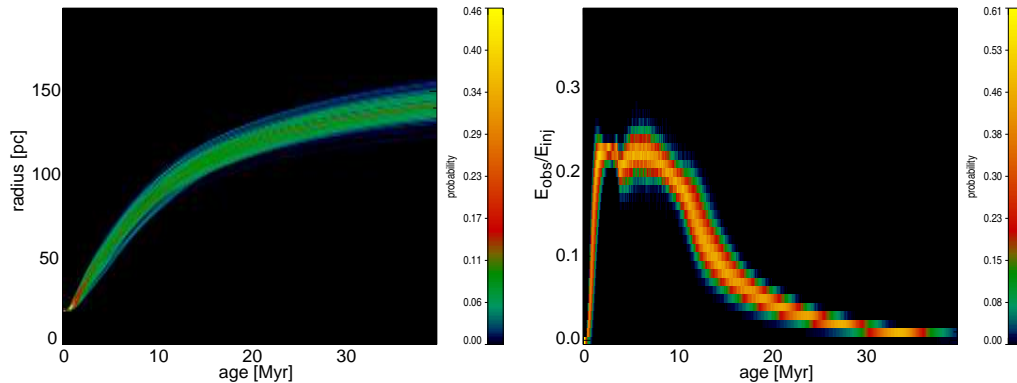


Fig. 2. Monte Carlo simulations of the evolution of the cavity created by clusters with 100 massive stars: The radius of the cavity blown by winds and supernovae is shown on the left. The figure on the right shows the ratio of radiated to injected kinetic energy, indicating the efficiency of cooling through X-ray emission. Colors illustrate probability densities, as in Fig. 1.

core-collapse supernovae. Here we discuss the possibility to recognize in stellar groups the typical ^{26}Al ejection time scale from WR stars and cc-SNe, respectively, through population synthesis analysis of the evolution of massive-star associations (Plüschke et al., 2000; Cervino et al., 2001).

2 Evolution of Massive-Star Groups

Massive stars are commonly formed in groups as a result of condensation of cores contained in giant molecular clouds with a typical mass around $10^5 M_{\odot}$ (e.g. Klessen, 2003). Energy feedback by newly-formed stars probably terminates the star formation process after a relatively short period, so that a “co-eval” group of stars will evolve. Radiation, winds, and supernovae of the most massive of these stars generates turbulence which can alter and possibly disrupt the parental molecular cloud on a time scale as short as 10^7 y. Turbulence may or may not sweep up cloud fragments to set up conditions for second-generation star formation. This general picture (see, e.g. Klessen, 2003; Matzner, 2002, and references therein) remains vague, so that (initial) conditions in specific stellar groups (mass of condensing GMC core, turbulent and magnetic-field energies, surrounding cloud filaments, ambient ISM density) are not accurately known. It is thus desirable to employ additional observational constraints, such as the ^{26}Al gamma-ray line map. For star forming regions with less than ~ 100 massive stars ($>8 M_{\odot}$), statistical effects must be taken into account (e.g., (Kretschmer, 2001; Cervino et al., 2001)).

Several open issues related to this picture are the subject of current studies: Injection of energy by massive stars should lead to heating of surrounding

material, observable as thermal X-ray emission. The emerging flux is sensitive to uncertain cooling of the hot cavity, which is strongly affected by evaporation of engulfed cloudlets and material on the wall of the bubble (Strickland and Stevens, 2000; de Avillez and Breitschwerdt, 2003). Ejection of nucleosynthesis products into the Galactic halo through “champagne flows” away from the region of the massive stars may temporarily reduce the overall rate of galactic chemical enrichment, but in the long run this matter is re-cycled by infall of halo clouds. The kinematics of high-velocity clouds (Wakker & Woerden, 1997) and their origin as well as galactic chemical evolution models with delayed infall are still quite uncertain (Silich and Tenorio-Tagle, 2001). The heating of gas and dust around massive stars should result in characteristic ionization/recombination features in spectra of diffuse galactic light as observed for distant galaxies; photoionization models suggest that the ionization of gas at intermediate latitudes is more efficient than expected from stratified ISM gas above the plane of the galaxy.

In order to address some of these issues, we developed a population synthesis code (Plüschke, 2001). Model ingredients are roughly similar to other current population synthesis codes: (1) A Salpeter Initial Mass Function sampled with Monte Carlo simulations with cutoffs at $8 M_{\odot}$ and $120 M_{\odot}$. (2) Stellar evolution quantities (lifetime through the cc-SN, wind and WR phases, ionizing luminosities, mass loss rates, etc) (taken from the Geneva group, Meynet et al., 1994). (3) Nucleosynthesis yields from hydrostatic and SN nucleosynthesis models and their ejection into the ISM (taken from Thielemann et al., 1996; Woosley et al., 1995). In addition, we compute the hydrostatic and thermal evolution of the surrounding ISM, from the injection of kinetic energy through winds and SNe, ionizing radiation and dust heating, and cooling through radiation and evaporation of wall material and engulfed cloudlets (following Shull and Saken, 1995). Products of the population-synthesis code include time profiles of the remaining star content, energy injection and radioactivity injection through winds and supernovae, ionizing radiation, and derived ISM cavity size(s) and X-ray luminosities (see Figures 1 and 2).

^{26}Al injection into the ISM (Figure 1 (left)) is characterized by a steep rise ~ 3.5 My after formation due to the most massive stars’ Wolf Rayet phases, ejecting core hydrogen-burning products via stellar winds, with a small contribution of cc-Type Ib/c SNe corresponding to the final stages of such massive stars. This is followed by a second peak due to the onset of cc-Type II SNe. The gradual descents from these prominent peaks are shaped by subsequently lower-mass stars with their correspondingly longer evolution time scales. After $\sim 12\text{--}15$ My the ^{26}Al gamma-ray emission from the stellar winds has ceased. Figure 1(right) shows that the injected kinetic energy is dominated by supernovae, because this practically does not depend on the stellar mass. This leads to the steady growth of the surrounding hot cavity as shown in Figure 2 (left). The thermalized energy of the bubble interior results in X-ray emission, due

to the high temperature of the cavity interior of $\sim 10^7$ K. The ratio between injected kinetic energy and radiated energy depends on the surrounding ISM: Both the evolution of the cavity through pdV work and ionization of cold cavity wall gas and engulfed cloudlets, as well as heating of the interior against radiative losses is driven by the energy injection into the cavity. The radiation efficiency reaches $\sim 25\%$ near the peak, when evaporation contributions are small ($\sim 10^{-4}$).

3 Interpretation of the Gamma-Ray Observations

One prominent target of nearby massive star studies is the Orion region: the Orion OB1 association at ~ 450 pc distance is a likely ^{26}Al source (Brown et al., 1995). From diffuse X-ray emission and HI measurements the existence and morphology of the “Eridanus” cavity in the ISM can be inferred. The Eridanus cavity extends from the edge of the local bubble over several 100 pc towards the Orion molecular clouds (Burrows et al., 1993). This cavity is bounded by dense neutral gas, its elongated shape attributed to the density structure of the local ISM in combination with stellar winds and supernovae from Orion OB1 stars as driving engines. The cavity age is estimated as 10 Myr (Brown et al., 1995), substantially longer than the ^{26}Al lifetime. We therefore assume that any ^{26}Al ejection from the younger Orion OB1 subgroups find this cavity already in existence, and hence the stellar ejecta from the latest Myrs expand into a pre-existing density structure. Therefore we expect ^{26}Al emission from Orion OB1 stars to be offset from the location of OB1 towards the Eridanus cavity. The proximity of the cavity and its consequently large angular extent allows us to search for the effect of “diffusion” of radioactive ejecta in the gamma-ray data, as gamma-ray telescopes typically have poor spatial resolution.

The COMPTEL 1.809 MeV map of the anticenter region (see Figure 3) indeed shows extended emission towards the south of the Orion molecular clouds. The peak is offset by about 12° from these clouds (Diehl et al., 2001). If prior massive star activity in this region produced the cavity which directed this recent ^{26}Al ejection into a funnel towards us and away from the Orion molecular clouds and the plane of the Galaxy, we expect such an offset of the ^{26}Al gamma-ray emission. ^{26}Al may be piling up against the nearest HI boundary wall of the cavity at ($l \sim 200^\circ$, $b \sim -15$ - -30°) (see Figures 3 and 4), and, combined with the decay of radioactive ^{26}Al while expanding into the cavity, could plausibly explain the observed emission structures.

From the population synthesis model and the known parameters of all (including the older) OB associations and subgroups in this region we constrain the history of star formation that shaped the region (Plüscke, 2001). Subgroup [b] of the OB1 association is found to have the right age to be responsible for

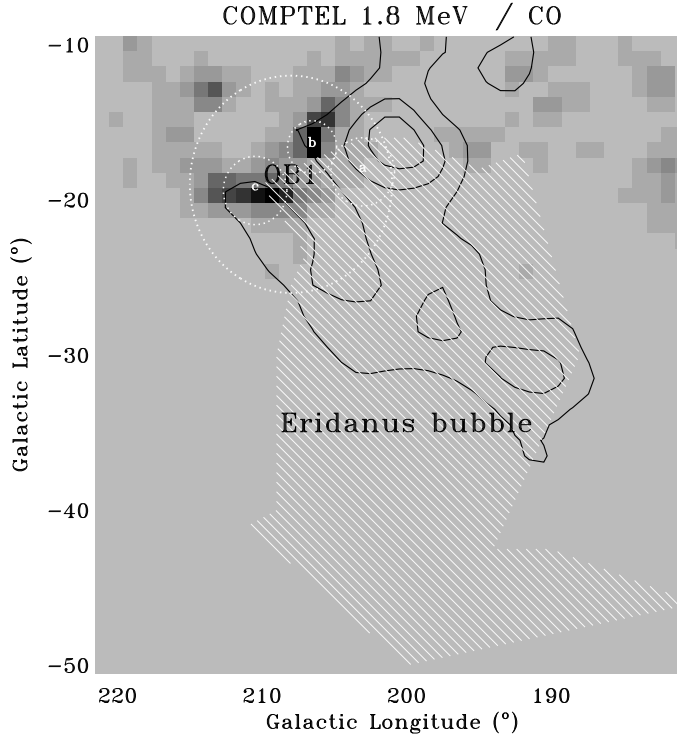


Fig. 3. The Orion region molecular clouds (grey), Eridanus cavity (hatched), and ^{26}Al emission (contours).

the bulk of the presently-observed ^{26}Al gamma-rays, while the oldest subgroup [a] may have been responsible for the formation of Eridanus cavity itself about 10–12 My ago.

The kinematics of the ^{26}Al ejection in this region is anisotropic. The flow of ^{26}Al is blocked at the far end by the Orion clouds, and directed towards us on the near side by the Eridanus cavity. ^{26}Al flow within the cavity should therefore lead to a net Doppler shift of the ^{26}Al gamma-ray line towards higher energies of ~ 0.1 keV, while ^{26}Al already deposited on cavity boundaries is \sim at rest. With Ge detector spectral resolution (3 keV FWHM for SPI on INTEGRAL, (Roques et al., 2003)) measurements of ^{26}Al emission from this region could test this scenario, thus complementing COMPTEL imaging.

4 Conclusions

The interaction of massive stars with their surroundings during the evolutionary time scale of a stellar association leads to specific observational effects: The injection of large amounts of kinetic energy capable to blow cavities of ~ 100 pc radius, or larger if the surrounding gas density is lower (as it is well above and below the galactic plane). Massive-star groups of different ages

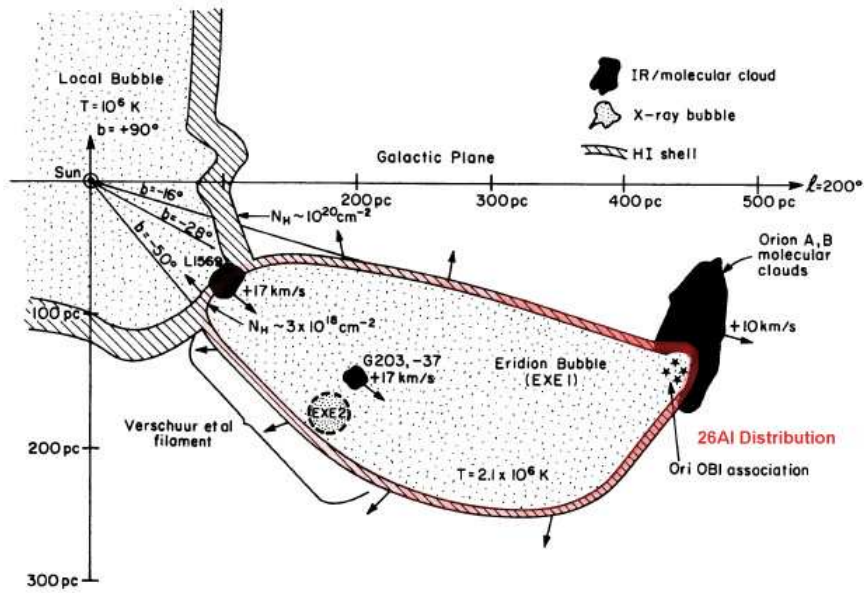


Fig. 4. The ^{26}Al emissivity from the Eridanus cavity, as it may be filled from the OB1 association. Although details of ^{26}Al propagation in the cavity are unknown, we expect SN ejecta and wind material to fill the cavity and be deposited on cavity boundaries, amounts reducing with source distance. The apparent ^{26}Al map corresponds to integrated ^{26}Al emission along lines of sight. (adapted from (Burrows et al., 1993))

find their surroundings pre-shaped into cavities and cloud fragments. Spatial correlations of ^{26}Al source tracers must account for such effects. In the nearby Orion/Eridanus region we find a significant offset between stars/tracers and gamma-ray line emission from ^{26}Al . This offset is consistent with the idea that ^{26}Al contained in stellar winds and SN ejecta can travel large distances in a few Myrs, especially when the outflow is directed into a pre-existing low density cavity.

Acknowledgements. This paper is based on several studies made with several colleagues and students. We thank in particular Stefan Plüschke for his contributions, and are grateful to Dieter Breitschwerdt, Jürgen Knödlseher, and Uwe Oberlack for useful discussions.

References

- Blaauw A. (1964), *Ann.Rev.Astr.Astroph.* **2**, 213
 Brown A.G.A. et al. (1995), *A&A* **300**, 903
 Burrows D.N. et al. (1993), *ApJ* **406**, 97
 Cerviño, M. et al. (2001) *A&A* **368**, 970
 de Avillez M.A., and Breitschwerdt D. (2003), *RevMexAA* **15**, 299
 de Zeeuw, P.W. et al. (1999), *AJ* **117**, 354

Diehl, R. et al. (1995), *A&A* **298**, 445
 Diehl, R. et al. (2001), *NewAstRev* **46**, 547
 Diehl, R. et al. (2003), *A&A* , (in press)
 Efremov Y., Elmegreen B.G. (1998), *MNRAS* **299**, 588
 Klessen, R.S. (2003), *Rev.Mod.Astr.*, **16**, 23
 Knödseder, J. (1999), *A&A* **344**, 68
 Knödseder J. (1999a), *ApJ* **510**, 915
 Knödseder J. *et al.* (1999), *A&A* **345**, 813
 Knödseder J. (2000), *A&A* **360**, 539
 Kretschmer K. (2001), Diploma Thesis, TU München
 Leising, M., & Clayton D.D. (1985), *ApJ* **294**, 591
 Mahoney, W. A. et al. (1982), *ApJ* **262**, 742
 Matzner, C. D. (2002) *ApJ*, 566, 302
 Meynet G., et al. (1995), *A&AS* **103**, 97
 Naya, J. E. et al. (1996), *Nature* **384**, 44
 Oberlack, U. et al. (2000), *A&A* **353**, 715
 Oberlack, U. (1997), Ph. D. Thesis, Technische Universität München
 Perrot C.A., Grenier I. (2003), *A&A* **404**, 519
 Plüschke, S. (2001), PhD Thesis, TU München, MPE Rep. 276
 Plüschke, S. et al. (2000), *AIP Conf. Proc.* **510**, 448
 Pöppel, W. (1997), *Fund. Cosm. Phys.* **18**, 1
 Prantzos, N., & Diehl, R. (1996), *Phys. Rep.* **267**, 1
 Roques, J.-P. et al. (2003), *A&A* , *submitted*
 Russeil, D. (2002), *IAU* **212**, 431
 Shull J., & Saken J. (1995), *ApJ* **444**, 663
 Silich, S. & Tenorio-Tagle, G. (2001) *ApJ*, 552, 91
 Smith, D. (2003), *ApJ* **589**, L55
 Smith, D. (2003), this volume
 Strickland, D. K. & Stevens, I. R. (2000) *M.N.R.A.S.*, 314, 511
 Thielemann, F.K., Nomoto, K. and Hashimoto, M. (1996), *ApJ*, **460**, 408
 van der Hucht, K. (2002), *IAU* **212**, 441
 Wakker B. & van Woerden H. (1997), *ARAA* **35**, 217
 Woosley, S.E. & Weaver, T.A. (1995), *ApJS* **101**, 181